EurJIC European Journal of Inorganic Chemistry

ChemPubSoc Europe

FULL PAPER

DOI:10.1002/ejic.201301171

Linear, Edge-Sharing Heterometallic Trinuclear [Co^{II}–Ln^{III}–Co^{II}] (Ln^{III} = Gd^{III}, Dy^{III}, Tb^{III}, and Ho^{III}) Complexes: Slow Relaxation of Magnetization in the Dy^{III} Derivative

Vadapalli Chandrasekhar,*[a,b] Sourav Das,[a] Atanu Dey,[a] Sakiat Hossain,[a] Subrata Kundu,[a] and Enrique Colacio*[c]

Keywords: Heterometallic complexes / Cobalt / Lanthanides / Magnetic properties / Ferromagnetic interactions / Schiff bases

The sequential reaction of a multisite coordination ligand (LH_4) with lanthanide (III) nitrates followed by the addition of $Co(NO_3)_2·6H_2O$ in a 4:1:2 ratio in the presence of triethylamine afforded a series of heterometallic, linear trinuclear complexes [$Co_2Ln(LH_3)_4$]·$3NO_3$ [Ln = Dy^{III} (**1**), Gd^{III} (**2**), Tb^{III} (**3**), and Ho^{III} (**4**)]. These tricationic complexes contain nitrate counteranions. The cationic portion of these complexes consists of three metal ions that are arranged in a linear fashion; a central Ln^{III} is present between the two terminal Co^{II} ions and is attached to the latter through two phenoxide bridging groups. This arrangement generates two contiguous four-membered $CoLnO_2$ rings. The Co^{II} ions are six-coordinate (2N, 4O) in a distorted octahedral geometry, whereas the central lanthanide ion is eight-coordinate (8O) in a distorted square-antiprismatic geometry. Magnetic studies of these complexes have been performed and indicate a slow relaxation of the magnetization for the Dy^{III} derivative **1**.

Introduction

The discovery that [$Mn_{12}O_{12}(OAc)_{16}(H_2O)_4$][1] is a single-molecule magnet (SMM), the magnetic behavior of which, below a critical temperature, resembles that of bulk magnets, has spurred extremely intense interdisciplinary research activity with participation from chemists, physicists, and materials scientists. The other types of molecular materials that have been discovered since include single-chain magnets[2] and single-ion magnets.[3] From the point of view of chemists, the excitement in this field has been the challenge to understand the structure–property relationships in these systems and to design and assemble various types of molecular systems that exhibit interesting magnetic behavior. On the basis of a qualitative understanding that the optimum requirements to extract SMM behavior from a system depends on a high ground-state spin, *S*, and a large magnetic anisotropy, *D*, several synthetic strategies were formulated to achieve these parameters.[4] Briefly, the strategies have been to synthesize polynuclear paramagnetic transition metal ion complexes [e.g., Mn(II/III),[5] Fe(II/III),[6] Co^{II},[7] or Ni^{II}[8]], lanthanide ion complexes of varying nuclearity (e.g., Ln_2,[9] Ln_3,[10] Ln_4,[11] Ln_5,[12] Ln_6),[13] and heterometallic 3d/4f complexes (e.g., Cu^{II}/Ln^{III},[14] Ni^{II}/Ln^{III},[15] Mn^{III}/Ln^{III}[16]). The latter, in particular, have attracted interest because appropriate 3d and 4f metal ions can interact favorably under suitable linkage conditions to generate interesting magnetic properties. Among the various systems that have been investigated, those containing Co^{II}/Ln^{III}[17] have not received as much attention, although, recent research on these compounds shows considerable promise. We have recently reported a dinuclear mixed-valent Co^{II}/Co^{III}[18] complex that exhibited slow relaxation of magnetization. Earlier, using a phosphorus-supported ligand, $SP[N(Me)N{=}CH{-}C_6H_3\text{-}2\text{-}OH\text{-}3\text{-}OMe]_3$ (LH_3), we have prepared several homo-[19] and heterometallic trinuclear complexes,[20] including $[L_2Co_2Ln]^+$ (Ln = Gd, Dy, Tb, Ho, and Eu),[17f,17g] many of which showed SMM behavior. Spurred by this, we were interested in preparing analogous compounds with a vastly different ligand system. Accordingly, herein, we report the synthesis, structural characterization, and magnetic behavior of [$Co_2Dy(LH_3)_4$]·$3NO_3$·2MeOH·$1.5H_2O$ (**1**), [$Co_2Gd(LH_3)_4$]·$3NO_3$·2MeOH·$0.5H_2O$ (**2**), [$Co_2Tb(LH_3)_4$]·$3NO_3$·2MeOH·$0.5H_2O$

[a] Department of Chemistry, Indian Institute of Technology Kanpur,
Kanpur 208016, India
E-mail: vc@iitk.ac.in
http://www.iitk.ac.in
[b] Tata Institute of Fundamental Research, Centre for Interdisciplinary Sciences,
21 Brundavan Colony, Narsingi, Hyderabad 500075, India
http://www.tifrh.res.in
[c] Departamento de QuímicaInorgánica, Facultad de Ciencias, Universidad de Granada,
Avenida de Fuentenueva s/n, 18071 Granada, Spain
E-mail: ecolacio@ugr.es
http://www.ugr.es

Supporting information for this article is available on the WWW under http://dx.doi.org/10.1002/ejic.201301171.

(**3**), and $[Co_2Ho(LH_3)_4]\cdot 3NO_3\cdot 2MeOH\cdot 0.5H_2O$ (**4**) prepared from 2-[2-hydroxy-3-(hydroxymethyl)-5-methylbenzylideneamino]-2-methylpropane1,3-diol (LH_4). The detailed magnetic studies for **1**–**4** indicate the presence of ferromagnetic behavior for the Dy^{III} (**1**) and Gd^{III} (**2**) analogues and a slow relaxation of magnetization for **1**.

Results and Discussion

Synthesis

The multisite coordination ligand LH_4 contains five binding sites: one phenolic oxygen atom, one benzyl alcohol oxygen atom, one imino nitrogen atom, and two hydroxy oxygen atoms. The sequential reaction of LH_4 with appropriate lanthanide salts followed by reaction with $Co(NO_3)_2\cdot 6H_2O$ in a 4:1:2 stoichiometric ratio in the presence of triethylamine afforded the trinuclear heterobimetallic compounds $[Co_2Ln(LH_3)_4]\cdot 3NO_3\cdot x MeOH\cdot y H_2O$ [Ln = Dy^{III}, x = 2, y = 1.5 (**1**); Ln = Gd^{III}, x = 2, y = 0.5 (**2**); Ln = Tb^{III}, x = 2, y = 0.5 (**3**); Ln = Ho^{III}, x = 2, y = 0.5 (**4**)], in good yields (>60%, see Exp. Section and Scheme 1). The ESI-MS spectra of **1**–**4** reveal that they retain their molecular integrity in solution as indicated by the presence of peaks at m/z = 430.08 corresponding to $[C_{52}H_{72}N_4O_{16}Co_2Dy]^{3+}$ for **1**, 428.09 corresponding to $[C_{52}H_{72}N_4O_{16}Co_2Gd]^{3+}$ for **2**, 428.41 corresponding to $[C_{52}H_{72}N_4O_{16}Co_2Tb]^{3+}$ for **3**, and 430.42 corresponding to $[C_{52}H_{72}N_4O_{16}Co_2Ho]^{3+}$ for **4**. The ESI-MS spectrum of **1**, as a representative example, is shown in Figure 1, and those of the others are in the Supporting Information (Figures S1–S3).

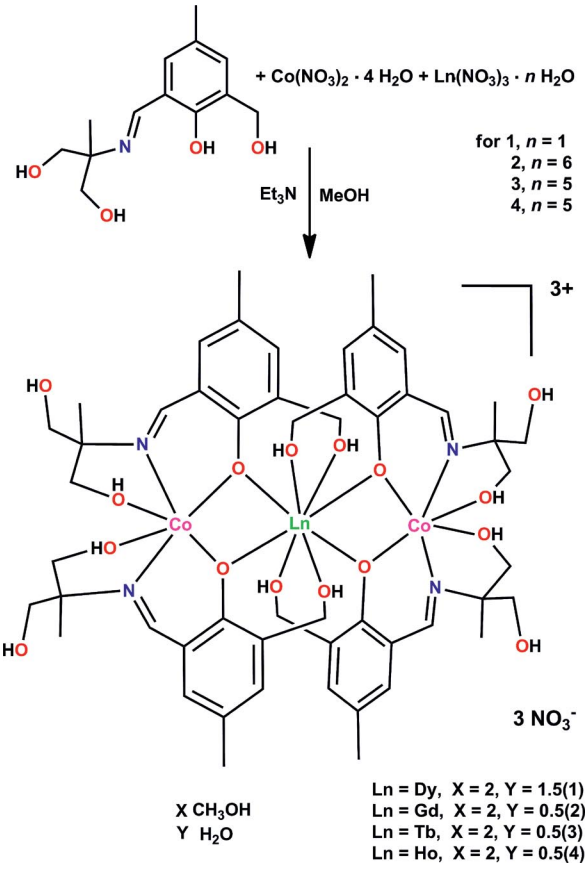

Scheme 1. Synthesis of the trinuclear heterometallic complexes **1**–**4**.

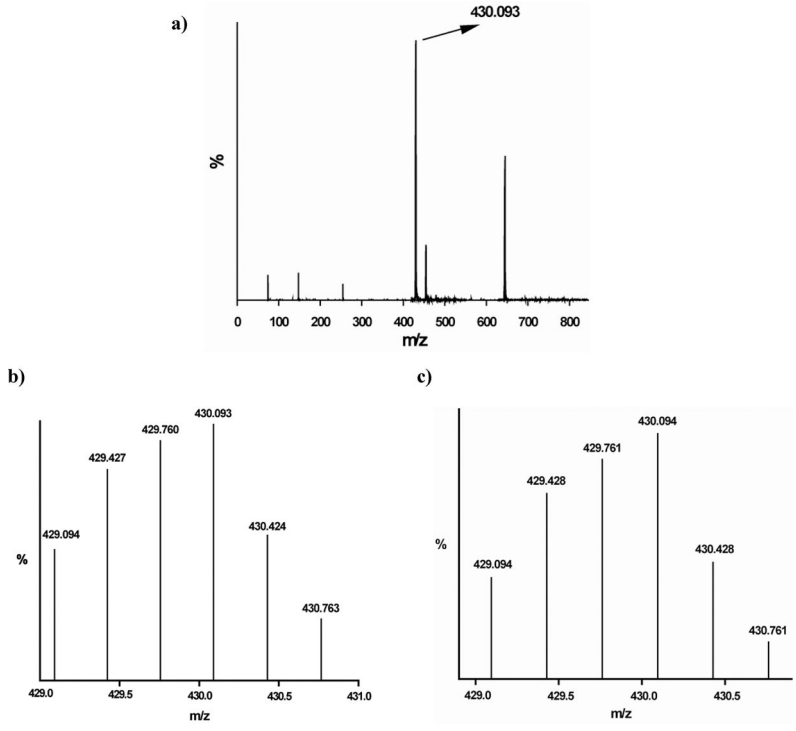

Figure 1. (a) Full range ESI-MS spectrum of **1**. (b) Experimental mass spectral pattern of the parent ion peak. (c) The simulated isotopic pattern for the parent ion peak shows a close resemblance with the experimental spectrum.

X-ray Crystallography

Single-crystal X-ray diffraction studies revealed that **1**–**4** are isostructural and crystallize in the monoclinic space group $P2_1/n$. All of the complexes are tricationic and contain three nitrate anions to neutralize the charge. In the following, the molecular structure of **1** will be described as a representative example to illustrate the common structural features of the four complexes. The molecular structure of **1** is shown in Figure 2; those of **2**–**4** are in the Supporting Information (Figure S4). Selected bond parameters of **1** are listed in the caption of Figure 2.

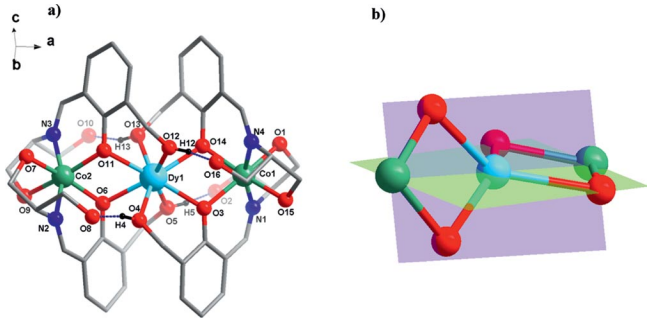

Figure 2. (a) The tricationic complex **1** (hydrogen atoms, methyl groups, and the solvent molecules have been omitted for clarity). Selected bond lengths [Å] and angles (°): Dy(1)–O(3) 2.344(7), Dy(1)–O(4) 2.390(7), Dy(1)–O(5) 2.410(6), Dy(1)–O(6) 2.349(5), Dy(1)–O(11) 2.334(5), Dy(1)–O(12) 2.382(6), Dy(1)–O(13) 2.399(7), Dy(1)–O(14) 2.321(6), Co(1)–N(1) 2.050(9), Co(1)–N(4) 2.079(9), Co(1)–O(1) 2.188(10), Co(1)–O(3) 2.072(7), Co(1)–O(14) 2.026(7), Co(1)–O(15) 2.127(13), Co(2)–N(2) 2.083(8), Co(2)–N(3) 2.061(8), Co(2)–O(6) 2.052(6), Co(2)–O(7) 2.130(7), Co(2)–O(9) 2.150(7), Co(2)–O(11) 2.035(6), Co(1)–O(3)–Dy(1) 104.6(3), Co(2)–O(6)–Dy(1) 104.9(2), Co(2)–O(11)–Dy(1) 106.0(2), Co(1)–O(14)–Dy(1) 106.9(3). (b) The trinuclear core of **1** showing the near orthogonal disposition of the two four-membered $CoDyO_2$ rings.

The heterometallic complex possesses a trinuclear $[Co_2Dy(\mu_2\text{-}O)_4]^{3+}$ core (Figure 2), which is assembled as a result of the cumulative coordination action of four singly deprotonated $[LH_3]^-$ ligands. Interestingly, only the phenolic proton is deprotonated, whereas the three $-CH_2OH$ groups that are present remain intact. Each $[LH_3]^-$ ligand uses a phenolate oxygen atom, an imino nitrogen atom, and the oxygen atoms of the benzyl alcohol and the $-NCH(CH_3)(CH_2OH)_2$ groups. One of the $-CH_2OH$ arms of the latter remains noncoordinating (Scheme 2). Each of the two terminal Co^{II} centers is surrounded by two $[LH_3]^-$ ligands and is bound by two phenolate oxygen atoms (O6 and O11), two imino nitrogen atoms (N2 and N3), and two CH_2OH units (O7 and O9) in a CoN_2O_4 coordination environment. The coordination geometry around the Co^{II} ion can be described as distorted octahedral (Figure 3, a). The central Dy^{III} ion has an overall 8O coordination environment in a square-antiprismatic geometry (Figure 3, b). All four $[LH_3]^-$ ligands in the complex are involved in binding. In addition to the four oxygen atoms from the benzyl alcohol groups (O4, O5, O12, and O13), four phenolate oxygen atoms (O3, O6, O11, and O14) are involved in coordination. Each of the terminal Co^{II} ions and the central Dy^{III} centers are bridged by two phenolate oxygen atoms to generate two four-membered $CoDyO_2$ rings, which are at an angle of 64.8(1)° with respect to each other (Figure 2, b). The bridging action of the phenolate oxygen atoms generates three contiguous polyhedra with common edges defined by O6/O11 and O3/O14 (Figure 4). Also, as result of the bridging phenolate coordination, the three metal ions are placed in a linear arrangement with a Co1–Dy1–Co2 bond angle of 177.9(1)°. The average Co^{II}–Dy^{III} distance is 3.495(1) Å, and the Co^{II}–Co^{II} distance is 6.990(2) Å. The linear arrangement of the metal ions can also be gauged when viewed along the Co–Dy–Co axis (Figure 5). As can be seen in Figure 5a, the four ligands involved in the assembly of **1** are organized symmetrically on the top and bottom of the trinuclear core. This arrangement can be contrasted with the paddle-wheel arrangement of the ligands in the previously described $[L_2CoLn]^+$ complexes (Figure 5, b). Complex **1** displays four strong intramolecular O–H···O hydrogen-bonding interactions between the benzyl alcohol oxygen atoms and the free $-CH_2OH$ arms (Figure 2).

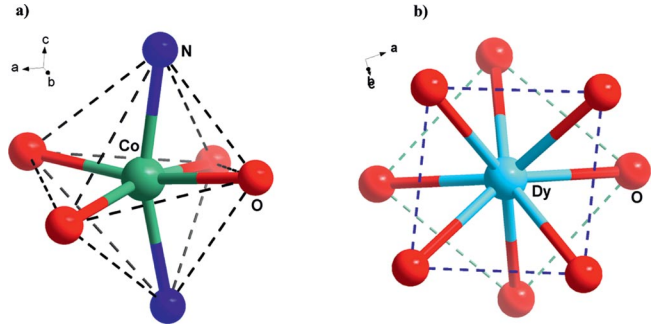

Figure 3. (a) Distorted octahedral geometry around the Co^{2+} ion. (b) Distorted square-antiprismatic geometry around the Dy^{3+} ion.

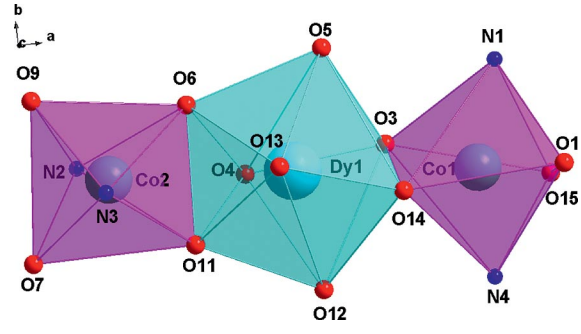

Figure 4. A view showing the edge-sharing of the three contiguous polyhedra.

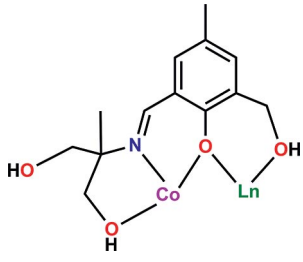

Scheme 2. Binding mode of LH_4.

Neighboring $[Co–Dy–Co]^{3+}$ cations are connected by hydrogen bonds involving coordinated hydroxymethyl groups and nitrate anions to give a 2D network in the *ac* plane. (Figure S5)

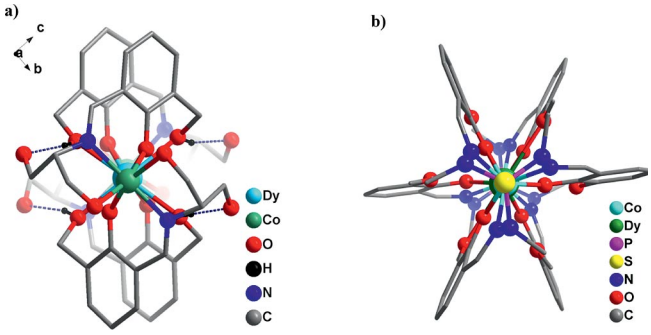

Figure 5. (a) The linear arrangement of the metal ions in **1**. (b) The literature example with a paddle-wheel arrangement of ligands about the Co–Ln–Co axis.[17f]

It is interesting to make a structural comparison of **1** with two other linear Co_2Ln complexes known in literature (Figures 5 and 6). Firstly, in the current instance, the tricationic complex assembly is accomplished through the use of four unsymmetrical Schiff base ligands featuring polyhydroxy and imino nitrogen atoms. The literature examples deal with monocationic complexes built from two symmetrical tripodal ligands containing imino nitrogen atoms and phenolate and methoxy oxygen atoms (Figure 6). Secondly, as shown in Figure 5b, the literature examples display a paddle-wheel arrangement of ligands about the Co–Ln–Co axis. In the present instance, the four ligands are arranged symmetrically in the top and bottom halves of the complex. Thirdly, the dihedral angles between the two $CoDyO_2$ rings in **1** is 64.8(3)°, whereas in the literature examples these angles are 59.7(14) and 61.4(2)°. The metric parameters involved in the current instance and in the literature examples are quite similar and are summarized in Table 1.

Magnetic Properties

The temperature dependence of $\chi_M T$ for **1**–**4** (χ_M is the molar magnetic susceptibility per Co_2Ln unit) in the temperature range 300–2 K range was measured with an applied magnetic field of 1000 Oe, and the results are displayed in Figure 7.

Let us to start with the Co–Gd complex **2**, the magnetic properties of which are easier to analyze. At room temperature, the $\chi_M T$ value for **2** of 14.47 $cm^3 mol^{-1} K$ is larger than that expected for two Co^{II} (S = 3/2) and one Gd^{III} (S = 7/2) ions that are not interacting (11.625 $cm^3 mol^{-1} K$ with g = 2), maybe because of both the orbital contribution of the Co^{II} ion (with an octahedral geometry and a $^4T_{1g}$ ground term) and the ferromagnetic interaction between the Co^{II} and Gd^{III} ions (see below). As the temperature de-

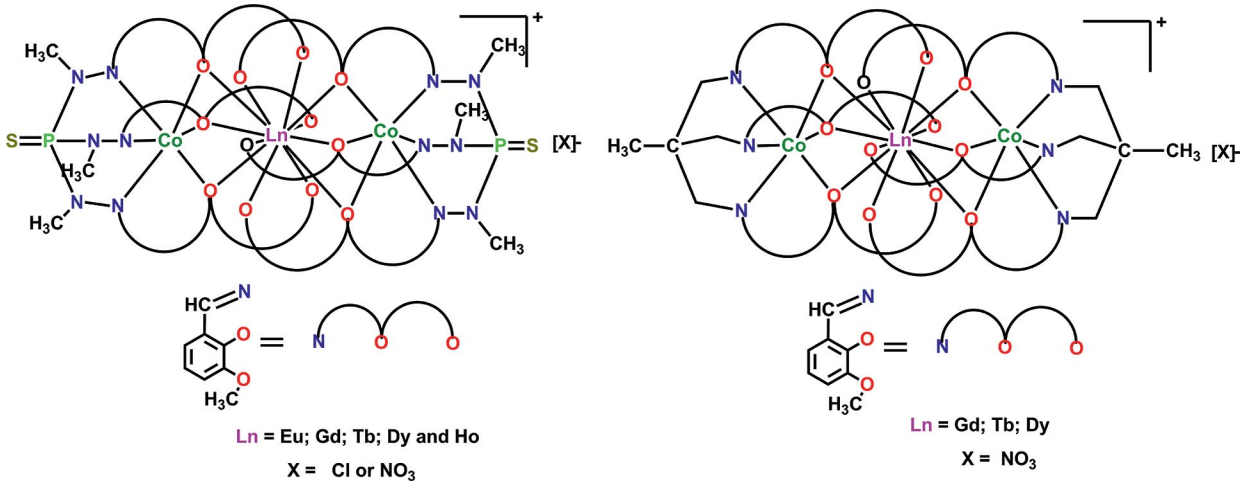

Figure 6. Two families of $[Co_2Ln]^+$ complexes known in literature.[17f,17g,17h]

Table 1. Comparison of bond lengths [Å] and angles [°] of the trinuclear $[Co^{II}–Ln^{III}–Co^{II}]$ complexes reported here and those reported previously (see Figure 6).

	$[(LH_3)_4Co_2Ln][NO_3]_3$	$[L_2Co_2Ln][NO_3]$[17h]	$[L_2Co_2Ln][NO_3]$[17f,17g]
$Co–N_{imine}$	2.035(11)–2.087(8)	2.087(6)–2.125(7)	2.096(6)–2.132(6)
$Co–O_{phenolic}$	2.026(6)–2.091(7)	2.057(6)–2.115(4)	2.076(4)–2.107(4)
$Co–O_{terminal\ hydroxo}$	2.126(8)–2.233(8)	–	–
$Ln–O_{phenolic}$	2.321(6)–2.378(7)	2.360(3)–2.456(5)	2.363(5)–2.396(3)
$Ln–O_{methoxy/benzyl\ hydroxide}$	2.382(6)–2.443(6)	2.868(4)–2.983(5)	2.865(3)–2.932(2)
Co–Ln	3.488(1)–3.508(2)	3.302(5)–3.321(1)	3.269(9)–3.310(9)
Co–Co	6.977(2)–7.023(2)	6.603(2)–6.634(4)	6.538(1)–6.621(1)
Co–Ln–Co	177.67(2)–177.99(3)	176.93(2)–178.41(5)	180.00(2)
Co–O–Ln	104.25(2)–106.51(2)	93.98(14)–95.40(2)	94.31(2)–94.43(2)

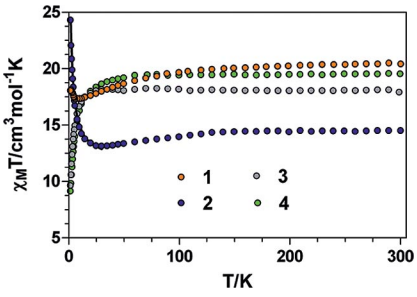

Figure 7. Temperature dependence of $\chi_M T$ for **1**–**4**. The solid line represents the best fit of the experimental data of **2** to the theoretical equation.

creases, the $\chi_M T$ value for **2** first slowly decreases from room temperature to reach a minimum value of 13.13 K $cm^3 mol^{-1} K$ at 30 K and then shows an abrupt increase to reach a value of 24.27 $cm^3 mol^{-1} K$ at 2 K. The observed high-temperature decrease is caused by the thermal depopulation of the spin–orbit coupling levels arising from the $^4T_{1g}$ ground term, whereas the increase at low temperature suggests a ferromagnetic interaction between the Co^{II} and Gd^{III} ions. The data for **2** were analyzed by considering that below 30 K only the lowest Kramer doublet of the Co^{II} ion with an effective spin $S_{eff} = 1/2$ is thermally populated. Although small differences between the bond angles and distances affect the two bridging fragments, for simplicity, we are going to consider the same exchange coupling for the Co^{II}–Gd^{III} interactions. This effective spin is related to the real spin by a factor of 5/3 and, therefore, the Hamiltonian that describes the magnetic exchange interaction between the Gd^{III} and Co^{II} ions is:[21]

$$\hat{S} = (5/3)\hat{S}_{eff}$$

$$\hat{H} = -J(\hat{S}_{Co1}\hat{S}_{Gd} + \hat{S}_{Co2}\hat{S}_{Gd}) - J_1(\hat{S}_{Co1} + \hat{S}_{Co2})$$
$$= -\frac{5}{3}J(\hat{S}_{Co1eff}\hat{S}_{Gd} + \hat{S}_{Co2eff}\hat{S}_{Gd}) - \frac{25}{9}J_1(\hat{S}_{Co1eff}\hat{S}_{Co2eff})$$

From this Hamiltonian, the molar magnetic susceptibility is calculated to be:

$$\chi_M = \frac{Ng^2\beta^2}{4kT}\frac{35 + 165\exp(16A) + 84\exp(7A) + 84\exp(9A - 25J_1/9kT)}{3 + 4\exp(7A) + 4\exp(9A - 25J_1/9kT) + 5\exp(16A)}$$

In this equation, $A = 5J/6kT$, and the same g value was assumed for all of the spin states. All attempts to fit the data to this equation were unsuccessful unless a term to account for the intermolecular interactions was included in the Hamiltonian. We used the molecular field approximation ($zJ' < S_z > \boldsymbol{S}_z$) to take into account such interactions. As J_1 only affects the energy of the $S = 7/2$ state with intermediate spin $S^* = S_{Co1} + S_{Co2} = 0$, this parameter cannot be accurately determined. In view of this and to avoid overparameterization, J_1 was fixed to zero. The best fit of the magnetic susceptibility data for $T < 30$ K to the theoretical equation

$$\chi_M' = \frac{\chi_M}{(1 - \frac{zJ'}{N\beta^2 g^2}\chi_M)}$$

was obtained for the following parameters: $J = +0.97(7)$, $g = 2.35(1)$ and $zJ' = 0.0047(1)$. Nevertheless, the extracted J value must be taken with caution and should be considered only as an approximate value because of the crudeness of the model, which does not take into account the following factors: (1) the contribution of upper levels, (2) the distortion from the octahedral symmetry of the Co^{II} coordination sphere, which leads to a highly anisotropic Kramer doublet ground state ($g_{\parallel} \neq g_{\perp}$), and (3) spin states with different g values. Nevertheless, it is worth noting that this approach allows the extraction of a J value for the Co–Gd–Co complex that is in agreement with values found by more complex ab initio calculations.[26] Moreover, the extracted J value is similar to those found for planar diphenoxo-bridged Co^{II}–Gd^{III} complexes containing a compartmental ligand ($J \approx +1$ cm^{-1})[22–25] but is larger than that observed for a trinuclear Co–Gd–Co complex bearing a tripodal ligand with three phenoxo bridges connecting Gd^{III} and Co^{II} ions and a folded $Gd(O)_2Co$ bridging fragment ($J = +0.52$).[17h] Experimental results on dinuclear Co^{II}–Gd^{III} complexes[22–24] and DFT calculations by us and others on di-μ-phenoxo dinuclear Gd–$(O)_2$–Cu[27] and Gd–$(O)_2$–Ni complexes[28] indicate that the ferromagnetic interaction between the M^{II} (Co, Cu, Ni) and Gd^{III} ions increases with the planarity of the M–O_2–Gd fragment and with the increase of the M–O–Gd angle. Therefore, the observed value for **2** is not unexpected as it exhibits a $Gd(O)_2Co$ planar fragment and large Gd–O–Co bridging angles. The magnetization isotherm of **2** at 2 K (Figure 8) shows a rapid increase at low field, in agreement with a high-spin state for this complex, and a rapid saturation of the magnetization that is almost complete at the maximum applied field of 5 T and reaches a value of 11.57 μ_B, close to that expected for the corresponding saturation value of 11.40 μ_B for $g_{Co} = 4.4$, $S_{effCo} = 1/2$, $g_{Gd} = 2.0$, and $S_{Gd} = 7/2$. In keeping with the ferromagnetic interaction observed for **2**, the experimental data are well above the Brillouin curve for two Co^{II} ($S_{eff} = 1/2$; $g = 4.4$) and one Gd^{III} ($g = 2.0$) ion that are not interacting.

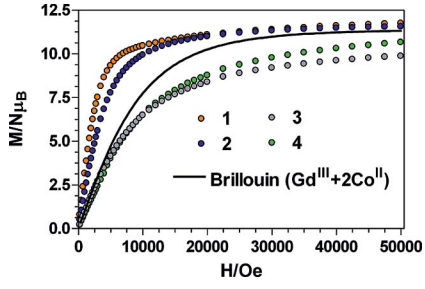

Figure 8. Field dependence of the magnetization at 2 K for **1**–**4**.

We now discuss the magnetic properties of **1**, **3**, and **4**. At room temperature, the $\chi_M T$ values for these complexes (20.37, 18.09, and 18.51 $cm^3 K$ mol^{-1}, respectively) are higher than those calculated (17.91, 15.56, and 17.81 $cm^3 K$

mol^{-1}, respectively) for two Co^{II} (S = 3/2 with g_{Co} = 2.0) and one Ln^{III} ion (Dy^{III} 4f^9, J = 15/2, S = 5/2, L = 5, $^6H_{15/2}$, g_J = 4/3; Tb^{III} 4f^8, J = 6, S = 3, L = 3, $^6F_7$, g_J = 3/2; Ho^{III}, L = 6, S = 2, J = 8, g_J = 5/4, $^5I_8$) that are not interacting in the free-ion approximation.

$$\chi_M T = \frac{N\beta^2}{3k}\left\{g_j^2 J(J+1) + 2g_{Co}^2 S(S+1)\right\}$$

These differences are mainly caused by the orbital contribution of the Co^{II} ions with an octahedral geometry and a $^4T_{1g}$ ground term and the possible ferromagnetic interactions between Co^{II} and Ln^{III} ions.

As the temperature decreases from room temperature, the $\chi_M T$ values for **1** steadily decreases to reach a minimum of 10.31 cm^3 mol^{-1} K at10 K. Below this temperature, $\chi_M T$ undergoes a sharp increase to reach a value of 18.02 cm^3 mol^{-1} K at 2 K. The decrease at high temperature is mainly caused by the depopulation of the Stark sublevels of the Dy^{III} ions, which arise from the splitting of the $^6H_{15/2}$ ground term by the ligand field as well as to the thermal depopulation of the levels that arises from spin–orbit coupling in the Co^{II} ions. The increase in $\chi_M T$ at low temperature indicates a ferromagnetic interaction between the Co^{II} and Dy^{III} ions, which is not unexpected in view of the planarity of the Co^{II}(diphenoxo)Dy^{III} bridging fragments. For **3** and **4**, as the temperature decreases, the $\chi_M T$ product decreases, first slightly to ca. 60–70 K and then sharply to reach values of 9.60 and 9.11 cm^3 K mol^{-1} at 2 K for **3** and **4**, respectively. This behavior is mainly caused by the thermal depopulation of the Stark sublevels of the Tb^{III} and Ho^{III} ions and the spin–orbit coupling levels in the Co^{II} ion. Therefore, it is not possible to know the sign of the magnetic exchange interaction in these compounds from the $\chi_M T$ versus T plot. It has been found experimentally that, for isostructural M–Ln complexes, the sign for the M^{II}–Tb^{III} and M^{II}–Ho^{III} (M^{II} = Co and Ni) magnetic exchange interactions is the same as that of the M^{II}–Gd^{III} interaction.[15e,17f–17h,24,25,27] In view of this, ferromagnetic interactions are expected for **3** and **4**.

The M versus H plot for **1** at 2 K (Figure 8) shows a relatively rapid increase in the magnetization at low field, in accord with a high-spin state for this complex, and a rapid saturation of the magnetization that is almost complete above 3 T and reaches a value of 11.75 $N\mu_B$. This behavior suggests the existence of a ground state well separated from the low-lying excited states that is stabilized by sufficiently large Co^{II}–Dy^{III} magnetic interactions. Nevertheless, the magnetization saturation value is far from the expected value (ca. 14.2 $N\mu_B$) for a Dy^{III} ion with strong easy-axis anisotropy (Ising spin at low temperature with J_z = ±15/2), ferromagnetically coupled with two S_{Coeff} = 1/2 ions with g_{Co} = 4.3. This may be because the most stable sublevels J_z of the Dy^{III} ions are not those with the highest value of J_z = ±15/2, which leads to a weaker anisotropy.

The field dependence of the magnetization at 2 K for **3** and **4** (Figure 8) reveals a relatively slow increase of the magnetization at low field compared to that of **1** and then a linear increase without clear saturation above 3 T. The linear high-field variation of the magnetization suggests the presence of a significant magnetic anisotropy (arising from the crystal-field effects on the free-ion ground state in the case of the Ln^{III} ion and from spin–orbit coupling in the case of the Co^{II} ions) and/or low-lying excited states that are partially [thermally and field-induced] populated. The presence of low-lying excited states close in energy to the ground state suggests that the magnetic exchange interactions for these compounds are weaker than that for **1**. The magnetization values for **3** and **4** at 5 T of 9.88 and 10.66 $N\mu_B$, respectively, are far from those expected for Tb^{III} and Ho^{III} ions (13.2 and 14.2 $N\mu_B$, respectively) with strong easy-axis anisotropy and J_z = ±6 (Tb^{III}) and ±8 (Ho^{III}) ground doublets ferromagnetically coupled with two S_{effCo} = 1/2 ions. In these cases, the sublevels with the highest ±J_z values should not be the lowest in energy and, therefore, the anisotropy is weaker.

Dynamic alternating current (ac) magnetic susceptibility measurements as a function of the temperature at different frequencies and under zero external field show that only **1** exhibits a slight frequency dependence of the out-of-phase (χ''_M) signals below ca. 10 K, typical of a thermally activated relaxation process (Figure S6), but does not reach a neat maximum, probably because there is an overlap with a faster quantum tunneling relaxation process, even at frequencies as high as 1400 Hz. This behavior seems to indicate that **1** exhibits slow relaxation of the magnetization and possibly SMM behavior. However, the χ''_M signal is quite weak with a χ''_M/χ'_M ratio of ca. 0.01. When the ac measurements were performed in the presence of a small external direct current (dc) field of 1000 G to fully or partly suppress the quantum tunneling relaxation of the magnetization (QTM), the intensity of the signals drastically increased but without resolution of any maximum in the χ''_M versus T plot, and the signals almost do not shift with respect to those observed at the same frequencies at zero field (Figure 9). The out-of-phase signals do not significantly shift with an applied field up to 2000 G (Figure S7).

Moreover, the signals undergo a sharp increase below ca. 5 K. All these facts seem to indicate that the quenching of the quantum tunneling of the magnetization by the field is almost negligible. The overlap between the thermally activated and QTM processes below 10 K precludes a detailed analysis of the former. QTM can be caused by the existence of intermolecular dipole–dipole interactions, which are known to mediate quantum tunneling relaxation processes. In some instances, this relaxation process cannot be shut down by the application of a static magnetic field, as in the case of **1**. An appropriate manner to try to eliminate the intermolecular interactions and, therefore, the QTM process would be to dilute the sample with an isostructural diamagnetic complex such as Zn^{II}–Y^{III}–Zn^{II}. These experiments are planned for the near future if we are able to cocrystallize the Co^{II}–Dy^{II}–Co^{II} complex with the isostructural diamagnetic Zn^{II}–Y^{III}–Zn^{II} complex.

Finally, it should be noted that there are other series of Co^{II}–Ln^{III}–Co^{II} complexes (Ln^{III} = Gd, Td, Dy, Ho), which were obtained with two different tripodal nonadadentate

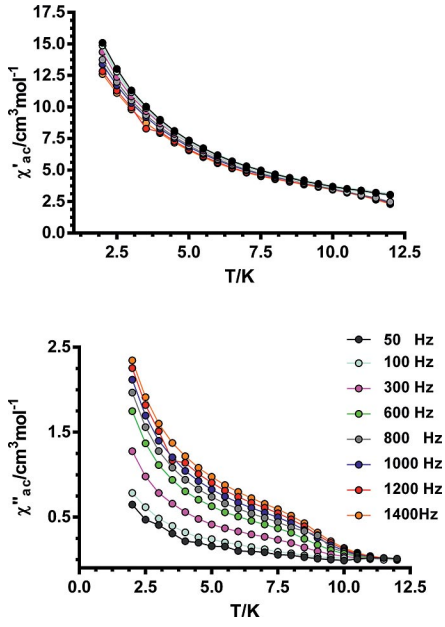

Figure 9. Temperature dependence of the in-phase χ'_M (top) and out-of-phase χ''_M (bottom) components of the ac susceptibility for **1** measured under 1000 Oe applied dc field.

ligands.[17f,17g,17h] In both series, the Co^{II} and Ln^{III} ions are connected by three phenoxo bridging groups with rather folded $Co(O)_3Ln$ bridging fragments. These compounds exhibit SMM behavior; in one of these series,[17h] this has been proved by hysteresis measurements below 1 K. However, with the exception of **1**, in our series no SMM behavior is observed. This may be caused by: (1) a comparatively weaker anisotropy of the Ln^{III} ions induced by ligand-field effects. The other two Co–Ln–Co series contain tripodal bridging ligands and exhibit LnO_{12} coordination spheres with six short $Ln–O_{phenoxo}$ distances and six long $Ln–O_{methoxy}$ distances, whereas the series described here has a square-prismatic LnO_8 coordination sphere formed by the coordination of four phenoxo and four hydroxy oxygen atoms. (2) The unfavorable orientation of the main local anisotropy axes of the Co^{II} and Ln^{III} ions leads to a relatively weak anisotropy for the whole molecule. Whereas **1**–**4** are not centrosymmetric and the diphenoxo-bridging fragments are turned from each other by 64.75°, (nonparallel main anisotropy axes of the Co^{II} ions) the complexes of the other two series are centrosymmetric (parallel main anisotropic axes of the Co^{II} ions). (3) The existence of a very efficient zero-field QTM. The extended 2D network of hydrogen bonds in **1**–**4** can facilitate the fast QTM relaxation process.

Conclusions

We have synthesized a series of linear trinuclear heterobimetallic compounds $[Co_2Ln(LH_3)_4]·3NO_3·xMeOH·yH_2O$ [Ln = Dy^{III}, x = 2, y = 1.5 (**1**); Ln = Gd^{III}, x = 2, y = 0.5 (**2**); Ln = Tb^{III}, x = 2, y = 0.5 (**3**); Ln = Ho^{III}, x = 2, y = 0.5 (**4**)] by using 2-[2-hydroxy-3-(hydroxymethyl)-5-methylbenzylideneamino]-2-methylpropane1,3-diol (LH_4). For **1**–**4**, dc measurements show ferromagnetic interactions at low temperatures. Dynamic magnetic (ac) measurements show that none of these compounds except **1** exhibits slow relaxation of the magnetization at zero applied field. For **1**, the application of external *dc* field, even up to 2000 G, does not suppress the fast zero-field QTM, and the intensity of the signals drastically increases without the observance of a maximum.

Experimental Section

Reagents and General Procedures: Solvents and other general reagents used in this work were purified according to standard procedures.[29] $Co(NO_3)_2·6H_2O$ and 2-amino-2-methylpropane-1,3-diol were obtained from S. D. Fine Chemicals, Mumbai, India. 2,6-Bis-(hydroxymethyl)-4-methylphenol, $Dy(NO_3)_3·H_2O$, $Ho(NO_3)_3·5H_2O$, $Tb(NO_3)_3·5H_2O$ $Gd(NO_3)_3·6H_2O$, and MnO_2 were obtained from Sigma Aldrich Chemical Co. and were used as received.

Instrumentation: Melting points were measured with a JSGW melting point apparatus. IR spectra were recorded with samples as KBr pellets with a Bruker Vector 22 FTIR spectrophotometer operating at 400–4000 cm^{-1}. Elemental analyses of the compounds were obtained with a Thermoquest CE instruments CHNS-O, EA/110 model analyzer. Electrospray ionization mass spectrometry (ESI-MS) spectra were recorded with a Micromass Quattro II triple quadrupole mass spectrometer. ^1H NMR spectra were recorded with samples in $CDCl_3$ solutions with a JEOL JNM LAMBDA 400 model spectrometer operating at 400.0 MHz; chemical shifts are reported in parts per million (ppm) and referenced with respect to internal tetramethylsilane (^1H).

Magnetic Measurements: The variable-temperature (2–300 K) magnetic susceptibility measurements on polycrystalline samples of **1**–**4** under an applied field of 1000 Oe were performed with a Quantum Design superconducting quantum interference device (SQUID) MPMS XL-5 device. The ac susceptibility measurements under different applied static fields were performed by using an oscillating ac field of 3.5 Oe and ac frequencies ranging from 1 to 1500 Hz. A pellet of the sample cut into very small pieces was placed in the sample holder to prevent any torquing of the microcrystals.

X-ray Crystallography: The crystal data for the compounds were collected with a Bruker SMART CCD diffractometer (Mo-K_α radiation, λ = 0.71073 Å). The program SMART[30a] was used for the collection of frames of data, indexing of reflections, and determination of the lattice parameters, SAINT[30a] was used for integration of the intensity of reflections and scaling, SADABS[30b] was used for absorption correction, and SHELXTL[30c,30d] was used for space-group and structure determination and least-squares refinements on F^2. All of the structures were solved by direct methods by using the program SHELXS-97[30e] and refined by full-matrix least-squares methods against F^2 with SHELXL-97.[30e] Hydrogen atoms were fixed at calculated positions, and their positions were refined by a riding model. All the non-hydrogen atoms were refined with anisotropic displacement parameters. The crystallographic figures were generated by using Diamond 3.1e software.[30f] The crystal data and the cell parameters for **1**–**4** are summarized in Table 2.

CCDC-945938 (for **1**), -945939 (for **2**), -945940 (for **3**), and -945941 (for **4**) contain the crystallographic data for this paper. These data can be obtained free of charge from the Cambridge Crystallographic Data Centre via www.ccdc.cam.ac.uk/data_request/cif.

Table 2. Crystal data and structure refinement parameters of **1**–**4**.

	1	**2**	**3**	**4**
Formula	$C_{108}H_{160}O_4Dy_2N_{14}O_{57}$	$C_{108}H_{160}Co_4Gd_2N_{14}O_{55}$	$C_{108}H_{160}Co_4N_{14}O_{55}Tb_2$	$C_{108}H_{160}Co_4Ho_2N_{14}O_{55}$
M [g]	3127.22	3084.72	3088.06	3100.08
Crystal system	monoclinic	monoclinic	monoclinic	monoclinic
Space group	$P2_1/n$	$P2_1/n$	$P2_1/n$	$P2_1/n$
a [Å]	15.013(5)	15.014(5)	15.059(5)	15.007(5)
b [Å]	22.564(5)	22.567(5)	22.522(5)	22.565(5)
c [Å]	20.165(5)	20.182(5)	20.168(5)	20.108(5)
β (°)	93.007(5)	93.093(5)	92.938(5)	93.046(5)
V [Å^3]	6822(3)	6828(3)	6831(3)	6800(3)
Z	2	2	2	2
$\rho_{calcd.}$ [g cm^{-3}]	1.522	1.500	1.501	1.514
μ [mm^{-1}]	1.651	1.524	1.588	1.719
$F(000)$	3204	3164	3168	3176
Crystal size [mm]	0.068 × 0.049 × 0.035	0.065 × 0.045 × 0.032	0.069 × 0.048 × 0.032	0.069 × 0.046 × 0.034
θ range [°]	4.14 –25.03	4.14–25.03	4.14–25.02	4.14–25.02
Limiting indices	–14 ≤ h ≤ 17 –26 ≤ k ≤ 26 –24 ≤ 1 ≤ 19	–17 ≤ h ≤ 12 –26 ≤ k ≤ 26 –20 ≤ l ≤ 24	–17 ≤ h ≤ 17 –26 ≤ k ≤ 26 –14 ≤ l ≤ 24	–17 ≤ h ≤ 17 –25 ≤ k ≤ 26 –23 ≤ l ≤ 13
Reflections collected	35199	35398	35152	35066
Independent reflections [R(int)]	11971 (0.0620)	11981 (0.0945)	11970 (0.0745)	11935 (0.0506)
Completeness to θ [%]	99.4	99.4	99.3	99.4
Refinement method	Full-matrix least-squares on F^2	Full-matrix least-squares on F^2	Full-matrix least-squares on F^2	Full-matrix least-squares on F^2
Data/restraints/ parameters	11971/55/876	11981/90/867	11970/79/837	11935/55/867
Goodness-of-fit on F^2	1.032	1.030	1.027	1.036
Final R indices [$I > 2\theta(I)$]	R_1 = 0.0792, wR_2 = 0.2159	R_1 = 0.0900, wR_2 = 0.2471	R_1 = 0.1060, wR_2 = 0.2752	R_1 = 0.0785, wR_2 = 0.2152
R indices (all data)	R_1 = 0.1142, wR_2 = 0.2458	R_1 = 0.1580, wR_2 = 0.2944	R_1 = 0.1586, wR_2 = 0.3136	R_1 = 0.1018, wR_2 = 0.2325
Largest diff. peak and hole [e Å^{-3}]	1.836 and –0.828	1.572 and –0.970	2.064 and –0.683	2.177 and –1.139

6-Formyl-2-(hydroxymethyl)-4-methylphenol: The following procedure has been used for the synthesis of the title compound and has been adapted from a previously published synthetic method.[31] A round-bottomed flask was charged with 2,6-bis(hydroxymethyl)-4-methylphenol (5 g, 30 mmol) and chloroform (500 mL). Manganese dioxide (16 g, 184 mmol) was added portionwise to the stirring solution. After 24 h, the reaction mixture was filtered, and the solvent was evaporated to give a crude product. This was purified by column chromatography with a silica gel column and EtOAc/*n*-hexane (1:9 v/v) as the eluant to yield a pale yellow solid, yield 2.88 g (58.3%), m.p. 72–74 °C, (ref. 74–76 °C).[32] $C_9H_{10}O_3$ (166.18): calcd. C 65.05, H 6.07; found C 65.09, H 6.16. ^{1}H NMR ($CDCl_3$): δ = 2.33 (s, 3 H), 4.72 (s, 2 H), 7.28 (s, 1 H), 7.39 (s, 1 H), 9.85 (s, 1 H), 11.16 (s, 1 H) ppm.

2-[2-Hydroxy-3-(hydroxymethyl)-5-methylbenzylideneamino]-2-methylpropane1,3-diol (LH_4): A methanolic solution of 2-(hydroxymethyl)-6-carbaldehyde-4-methylphenol (1.01 g, 6.07 mmol) was added dropwise to a stirred solution of 2-amino-2-methylpropane-1,3-diol (0.63 g, 6.00 mmol) in methanol (30 mL) at room temperature. After the addition was over, the reaction mixture was heated under reflux for 6 h. Then, the reaction mixture was cooled to room temperature, and most of the solvent was removed with a rotary evaporator with gentle heating. The concentrate thus obtained (10 mL) was kept in a refrigerator at 5 °C. The bright yellow crystalline material obtained was collected by suction filtration, washed with a small amount of cold methanol, and air-dried, yield 1.32 g (85.89%), m.p. 100 °C. $C_{13}H_{19}NO_4$ (253.30): calcd. C 61.64, H 7.56, N 5.53; found C 61.76, H 7.52, N 5.66. ^{1}H NMR ($CDCl_3$): δ = 1.14 (s, 3 H), 2.21 (s, 3 H), 3.42 (s, 6 H), 4.46 (s, 2 H), 7.07 (s, 1 H), 7.17 (s, 1 H), 8.41 (s, 1 H) ppm. ESI-MS: m/z = 254.14 [M + H]$^+$.

General Procedure for the Synthesis of Metal Complexes 1–4: A general procedure was applied for the preparation of **1**–**4**. To a stirred solution of LH_4 in methanol (30 mL), $Ln(NO_3)_3{\cdot}nH_2O$ (For **1**, n = 1; **2**, n = 6; **3**, n = 5; **4**, n = 5) was added. Then, triethylamine was added to the above solution, and the reaction mixture was stirred for 15 minutes. After this, a methanolic solution of $Co(NO_3)_2{\cdot}6H_2O$ was added dropwise. The resulting red-brown solution was stirred for a further 12 h to afford a clear solution. This solution was filtered, and the filtrate was evaporated to dryness. The residue obtained was washed with diethyl ether, dried, dissolved in methanol/chloroform (1:1), and kept for crystallization. After 4–7 d, a pure crystalline product suitable for X-ray diffraction was isolated. Specific details of each reaction and the characterization data of the products obtained are given below.

$[Co_2Dy(LH_3)_4]{\cdot}3NO_3{\cdot}2MeOH{\cdot}1.5H_2O$ (1): Quantities: $Co(NO_3)_2{\cdot}6H_2O$ (0.04 g, 0.14mmol), $Dy(NO_3)_3{\cdot}H_2O$ (0.03g, 0.07 mmol), LH_4 (0.08 g, 0.29 mmol), and Et_3N (0.06 mL, 0.59 mmol), yield 0.069 g, 63% (based on Dy), m.p. >260 °C. IR (KBr): $\tilde{\nu}$ = 3196 (b), 2928 (w), 2881 (w), 1632 (s), 1568 (s), 1454 (s), 1384 (s), 1294 (s), 1267 (s), 1171 (w), 1152 (s), 1047 (s), 999 (w), 975 (w), 818 (w), 794 (w), 692 (w), 579 (w) cm^{-1}. ESI-MS: m/z = 430.08 [$C_{52}H_{72}N_4O_{16}Co_2Dy$]$^{3+}$. $C_{54}H_{83}Co_2DyN_7O_{28.5}$ (1566.63): calcd. C 41.40, H 5.34, N 6.26; found C 41.52, H 5.23, N 6.32.

$[Co_2Gd(LH_3)_4]{\cdot}3NO_3{\cdot}2MeOH{\cdot}0.5H_2O$ (2): Quantities: $Co(NO_3)_2{\cdot}6H_2O$ (0.04 g, 0.14 mmol), $Gd(NO_3)_3{\cdot}6H_2O$ (0.03 g, 0.07 mmol), LH_4 (0.08 g, 0.29 mmol), and Et_3N (0.06 mL, 0.59 mmol), yield 0.062 g, 66% (based on Gd), m.p. >260 °C. IR (KBr): $\tilde{\nu}$ = 3211 (b), 2928 (w), 2881 (w), 1632 (s), 1567 (s), 1453 (s), 1384 (s), 1293 (s), 1243 (s), 1172 (w), 1047 (s), 997 (w), 974 (w), 818 (w), 794 (w), 693 (w), 579 (w) cm^{-1}. ESI-MS: m/z = 428.09 [$C_{52}H_{72}N_4O_{16}Co_2$-

Gd]$^{3+}$. $C_{54}H_{81}Co_2GdN_7O_{27.5}$ (1543.37): calcd. C 42.02, H 5.29, N 6.35; found C 42.31, H 5.18, N 6.43.

$[Co_2Tb(LH_3)_4]\cdot 3NO_3\cdot 2MeOH\cdot 0.5H_2O$ (3): Quantities: $Co(NO_3)_2\cdot 6H_2O$ (0.04 g, 0.14 mmol), $Tb(NO_3)_3\cdot 5H_2O$ (0.03 g, 0.07 mmol), LH_4 (0.08 g, 0.29 mmol), and Et_3N (0.06 mL, 0.59 mmol), yield 0.071 g, 64% (based on Tb), m.p. >260 °C. IR (KBr): $\tilde{\nu}$ = 3198 (b), 2929 (w), 2888 (w), 1632 (s), 1567 (s), 1453 (s), 1386 (s), 1294 (s), 1242 (s), 1150 (w), 1046 (s), 999 (w), 975 (w), 820 (w), 794 (w), 693 (w), 580 (w) cm^{-1}. ESI-MS: *m/z* = 428.41 [$C_{52}H_{72}N_4O_{16}Co_2$-Tb]$^{3+}$. $C_{54}H_{81}Co_2N_7O_{27.5}Tb$ (1544.31): calcd. C 41.98, H 5.28, N 6.35; found C 42.21, H 5.15, N 6.41.

$[Co_2Ho(LH_3)_4]\cdot 3NO_3\cdot 2MeOH\cdot 0.5H_2O$ (4): Quantities: $Co(NO_3)_2\cdot 6H_2O$ (0.04 g, 0.14 mmol), $Ho(NO_3)_3\cdot 5H_2O$ (0.03 g, 0.07 mmol), LH_4 (0.08 g, 0.29 mmol), and Et_3N (0.06 mL, 0.59 mmol), yield 0.068 g, 61% (based on Ho), m.p. >260 °C. IR (KBr): $\tilde{\nu}$ = 3220 (b), 2924 (w), 2882 (w), 1632 (s), 1567 (s), 1454 (s), 1384 (s), 1294 (s), 1224 (s), 1171 (w), 1048 (s), 998 (w), 974 (w), 819 (w), 794 (w), 693 (w), 578 (w) cm^{-1}. ESI-MS: *m/z* = 430.42 [$C_{52}H_{72}N_4O_{16}Co_2$-Ho]$^{3+}$. $C_{54}H_{81}Co_2HoN_7O_{27.5}$ (1550.31): calcd. C 41.82, H 5.26, N 6.32; found C 42.13, H 5.12, N 6.45.

Supporting Information (see footnote on the first page of this article): ESI-MS, tricationic portion of **2**–**4**, hydrogen-bond 2D network for **1**, H-bonding for **1**, list of bond lengths and angles, temperature dependece of the AC susceptibility for complex **1** at zero field, and field dependence of the out-of-phase component at 1200 Hz.

Acknowledgments

The authors are thankful to the Department of Science and Technology (DST), New Delhi, for financial support. S. D., A. D., S. H. and S. K. thank the Council of Scientific and Industrial Research (CSIR), New Delhi for Senior Research Fellowships. V. C. is thankful to the Department of Science and Technology for a J. C. Bose National Fellowship. E. C. thanks the Spanish Ministerio de Ciencia e Innovación (MICINN) (project number CTQ-2011-24478), the Junta de Andalucia (FQM-195 and Project of excellence, P11-FQM-7756), and the University of Granada for financial support.

[1] a) D. Gatteschi, R. Sessoli, J. Villain, *Molecular Nanomagnets*, Oxford University Press, Oxford, UK, **2006**; b) R. Sessoli, L. Hui, A. R. Schake, S. Wang, J. B. Vincent, K. Folting, D. Gatteschi, G. Christou, *J. Am. Chem. Soc.* **1993**, *115*, 1804.

[2] a) H. Miyasaka, T. Madanbashi, A. Saitoh, N. Motokawa, R. Ishikawa, M. Yamashita, S. Bahr, W. Wernsdorfer, R. Clerac, *Chem. Eur. J.* **2012**, *18*, 3942; b) J. Boeckmann, C. Nather, *Chem. Commun.* **2011**, *47*, 7104; c) T. S. Venkatakrishnan, S. Sahoo, N. Brefuel, C. Duhayon, C. Paulsen, A.-L. Barra, S. Ramasesha, J.-P. Sutter, *J. Am. Chem. Soc.* **2010**, *132*, 6047; d) T. D. Harris, M. V. Bennett, R. Clerac, J. R. Long, *J. Am. Chem. Soc.* **2010**, *132*, 3980; e) X. Feng, T. D. Harris, J. R. Long, *Chem. Sci.* **2011**, *2*, 1688; f) E. Pardo, C. Train, R. Lescouezec, Y. Journaux, J. Pasan, C. Ruiz-Perez, F. S. Delgado, R. Ruiz-Garcia, F. Lloret, P. Carley, *Chem. Commun.* **2010**, *46*, 2322.

[3] a) D. E. Freedman, W. H. Harman, T. D. Harris, G. J. Long, C. J. Chang, J. R. Long, *J. Am. Chem. Soc.* **2010**, *132*, 1224; b) S.-D. Jiang, B.-W. Wang, H.-L. Sun, Z.-M. Wang, S. Gao, *J. Am. Chem. Soc.* **2011**, *133*, 4730; c) J. Vallejo, I. Castro, R. Ruiz-Garcia, J. Cano, M. Julve, F. Lloret, G. De Munno, W. Wernsdorfer, E. Pardo, *J. Am. Chem. Soc.* **2012**, *134*, 15704; d) J. M. Zadrozny, J. R. Long, *J. Am. Chem. Soc.* **2011**, *133*, 20732; e) D. Weismann, Y. Sun, Y. Lan, G. Wolmershäuser, A. K. Powell, H. Sitzmann, *Chem. Eur. J.* **2011**, *17*, 4700; f) T. Jurca, A. Farghal, P.-H. Lin, I. Korobkov, M. Murugesu, D. S. Richardson, *J. Am. Chem. Soc.* **2011**, *133*, 15814; g) N. Ishikawa, M. Sugita, T. Ishikawa, S. Koshihara, S. Kaizu, *J. Phys. Chem. B* **2004**, *108*, 11265; h) M. A. Aldamen, J. M. Clemente-Juan, E. Coronado, C. Martí-Gastaldo, A. Gita-Ariño, *J. Am. Chem. Soc.* **2008**, *130*, 8874; i) J. Ruiz, A. J. Mota, A. Rodríguez-Diéguez, S. Titos, J. M. Herrera, E. Ruiz, E. Cremades, J. P. Costes, E. Colacio, *Chem. Commun.* **2012**, *48*, 7916.

[4] a) S. Hill, R. S. Edwards, N. Aliaga-Alcalde, G. Christou, *Science* **2003**, *302*, 1015; b) A. L. Barra, D. Gatteschi, R. Sessoli, *Phys. Rev. B* **1997**, *56*, 8192; c) R. Sessoli, A. K. Powell, *Coord. Chem. Rev.* **2009**, *253*, 2328; d) W. Wernsdorfer, *Adv. Chem. Phys.* **2001**, *118*, 99; e) D. Gatteschi, A. Caneschi, L. Pardi, R. Sessoli, *Science* **1994**, *265*, 1054.

[5] a) G. Christou, *Polyhedron* **2005**, *24*, 2065; b) C. J. Milios, R. Inglis, A. Vinslava, R. Bagai, W. Wernsdorfer, S. Parsons, S. P. Perlepes, G. Christouand, E. K. Brechin, *J. Am. Chem. Soc.* **2007**, *129*, 12505; c) A. M. Ako, I. J. Hewitt, V. Mereacre, R. Clerac, W. Wernsdorfer, C. E. Anson, A. K. Powell, *Angew. Chem.* **2006**, *118*, 5048; *Angew. Chem. Int. Ed.* **2006**, *45*, 4926; d) T. Taguchi, W. Wernsdorfer, A. Abboud, G. K. Christou, *Inorg. Chem.* **2010**, *49*, 199; e) Y.-G. Li, W. Wernsdorfer, R. Clérac, I. J. Hewitt, C. E. Anson, A. K. Powell, *Inorg. Chem.* **2006**, *45*, 2376.

[6] a) T. K. Prasad, G. Poneti, L. Sorace, M. J. Rodriguez-Douton, A. L. Barra, P. Neugebauer, L. Costantino, R. Sessoli, A. Cornia, *Dalton Trans.* **2012**, *41*, 8368; b) C. Schlegel, E. Burzurí, F. Luis, F. Moro, M. Manoli, E. K. Brechin, M. Murrie, J. V. Slageren, *Chem. Eur. J.* **2010**, *16*, 10178; c) R. Bagai, W. Wernsdorfer, K. A. Abboud, G. Christou, *J. Am. Chem. Soc.* **2007**, *129*, 12918; d) Y. Y. Zhu, X. Guo, C. Cui, B. W. Wang, Z. M. Wang, S. Gao, *Chem. Commun.* **2011**, *47*, 8049; e) A. M. Ako, V. Mereacre, Y. H. Lan, W. Wernsdorfer, R. Clérac, C. E. Anson, A. K. Powell, *Inorg. Chem.* **2010**, *49*, 1.

[7] a) M. Murrie, *Chem. Soc. Rev.* **2010**, *39*, 1986 and references cited therein; b) A. Ferguson, A. Parkin, J. Sanchez-Benitez, K. Kamenev, W. Wernsdorfer, M. Murrie, *Chem. Commun.* **2007**, 3473; c) B. Moubaraki, K. S. Murray, T. A. Hudson, R. Robson, *Eur. J. Inorg. Chem.* **2008**, 4525; d) K. W. Galloway, A. M. Whyte, W. Wernsdorfer, J. Sanchez-Benitez, K. V. Kamenev, A. Parkin, R. D. Peacock, M. Murrie, *Inorg. Chem.* **2008**, *47*, 7438; e) M. H. Zeng, M. X. Yao, H. Liang, W. X. Zhang, X. M. Chen, *Angew. Chem.* **2007**, *119*, 1864; *Angew. Chem. Int. Ed.* **2007**, *46*, 1832.

[8] a) A. K. Bouldalis, M. Pissas, C. P. Raptopoulou, V. Psycharis, B. Abarca, R. Ballesteros, *Inorg. Chem.* **2008**, *47*, 10674; b) S. Petit, P. Neugebauer, G. Pilet, G. Chastanet, A. L. Barra, A. B. Antunes, W. Wernsdorfer, D. Luneau, *Inorg. Chem.* **2012**, *51*, 6645; c) A. Ferguson, J. Lawrence, A. Parkin, J. Sanchez-Benitez, K. V. Kamenev, E. K. Brechin, W. Wernsdorfer, S. Hill, M. Murrie, *Dalton Trans.* **2008**, 6409; d) A. Bell, G. Aromi, S. J. Teat, W. Wernsdorfer, R. E. P. Winpenny, *Chem. Commun.* **2005**, 2808.

[9] a) P. H. Lin, T. J. Burchell, R. Clérac, M. Murugesu, *Angew. Chem.* **2008**, *120*, 8980; *Angew. Chem. Int. Ed.* **2008**, *47*, 8848; b) G. F. Xu, Q. L. Wang, P. Gamez, Y. Ma, R. Clérac, J. K. Tang, S. P. Yan, P. Cheng, D. Z. Liao, *Chem. Commun.* **2010**, *46*, 1506; c) R. A. Layfield, J. J. W. McDouall, S. A. Sulway, F. Tuna, D. Collison, R. E. P. Winpenny, *Chem. Eur. J.* **2010**, *16*, 4442.

[10] a) I. J. Hewitt, Y. Lan, C. E. Anson, J. Luzon, R. Sessoli, A. K. Powell, *Chem. Commun.* **2009**, 6765; b) J. Luzon, K. Bernot, I. J. Hewitt, C. E. Anson, A. K. Powell, R. Sessoli, *Phys. Rev. Lett.* **2008**, *100*, 247205; c) M. U. Anwar, S. S. Tandon, L. N. Dawe, F. Habib, M. Murugesu, L. K. Thompson, *Inorg. Chem.* **2012**, *51*, 1028; d) F. S. Guo, J. L. Liu, J. D. Leng, Z. S. Meng, Z. J. Lin, M. L. Tong, S. Gao, L. Ungur, L. F. Chibotaru, *Chem. Eur. J.* **2011**, *17*, 2458.

[11] a) Y. Bi, X.-T. Wang, W. Liao, X. Wang, R. Deng, H. Zhang, S. Gao, *Inorg. Chem.* **2009**, *48*, 11743; b) H.-S. Ke, G.-F. Xu, Y.-

N. Guo, P. Gamez, C. M. Beavers, S. J. Teat, J. K. Tang, *Chem. Commun.* **2010**, *46*, 6057; c) Y. N. Guo, G. F. Xu, P. Gamez, L. Zhao, S. Y. Lin, R. P. Deng, J. K. Tang, H. J. Zhang, *J. Am. Chem. Soc.* **2010**, *132*, 8538; d) S. Y. Lin, L. Zhao, H. Ke, Y. N. Guo, J. K. Tang, Y. Guoa, J. Dou, *Dalton Trans.* **2012**, *41*, 3248; e) G. Abbas, Y. Lan, G. E. Kostakis, W. Wernsdorfer, C. E. Anson, A. K. Powell, *Inorg. Chem.* **2010**, *49*, 8067; f) V. Chandrasekhar, S. Hossain, S. Das, S. Biswas, J. P. Sutter, *Inorg. Chem.* **2013**, *52*, 6346.

[12] a) M. T. Gamer, Y. Lan, P. W. Roesky, A. K. Powell, R. Clérac, *Inorg. Chem.* **2008**, *47*, 6581; b) J. B. Peng, X. J. Kong, Y. P. Ren, L. S. Long, R. B. Huang, L. S. Zheng, *Inorg. Chem.* **2012**, *51*, 2186; c) R. J. Blagg, C. A. Muryn, E. J. L. McInnes, F. Tuna, R. E. P. Winpenny, *Angew. Chem.* **2011**, *123*, 6660; *Angew. Chem. Int. Ed.* **2011**, *50*, 6530.

[13] a) B. Hussain, D. Savard, T. J. Burchell, W. Wernsdorfer, M. Murugesu, *Chem. Commun.* **2009**, 1100; b) I. J. Hewitt, J. K. Tang, N. T. Madhu, C. E. Anson, Y. Lan, J. Luzon, M. Etienne, R. Sessoli, A. K. Powell, *Angew. Chem.* **2010**, *122*, 6496; *Angew. Chem. Int. Ed.* **2010**, *49*, 6352; c) S. Xue, L. Zhao, Y. N. Guo, P. Zhang, J. K. Tang, *Chem. Commun.* **2012**, *48*, 8946; d) Y. N. Guo, X. H. Chen, S. Xue, J. K. Tang, *Inorg. Chem.* **2012**, *51*, 4035; e) H. Tian, M. Wang, L. Zhao, Y. N. Guo, Y. Guo, J. K. Tang, Z. Liu, *Chem. Eur. J.* **2012**, *18*, 442.

[14] a) G. Novitchi, G. Pilet, L. Ungur, V. V. Moshchalkov, W. Wernsdorfer, L. F. Chibotaru, D. Luneau, A. K. Powell, *Chem. Sci.* **2012**, *3*, 1169; b) S. K. Langley, L. Ungur, N. F. Chilton, B. Moubaraki, L. F. Chibotaru, K. S. Murray, *Chem. Eur. J.* **2011**, *17*, 9209; c) G. Novitchi, W. Wernsdorfer, L. F. Chibotaru, J.-P. Costes, C. E. Anson, A. K. Powell, *Angew. Chem.* **2009**, *121*, 1642; *Angew. Chem. Int. Ed.* **2009**, *48*, 1614; d) F. Mori, T. Nyui, T. Ishida, T. Nogami, K.-Y. Choi, H. Nojiri, *J. Am. Chem. Soc.* **2006**, *128*, 1440; e) V. Chandrasekhar, A. Dey, S. Das, M. Rouziéres, R. Clérac, *Inorg. Chem.* **2013**, *52*, 2588.

[15] a) C. G. Efthymiou, T. C. Stamatatos, C. Papatriantafyllopoulou, A. J. Tasiopoulos, W. Wernsdorfer, S. P. Perlepes, G. Christou, *Inorg. Chem.* **2010**, *49*, 9737; b) T. D. Pasatoiu, J.-P. Sutter, A. M. Madalan, F. Z. C. Fellah, C. Duhayon, M. Andruh, *Inorg. Chem.* **2011**, *50*, 5890; c) K. Xiong, X. Wang, F. Jiang, Y. Gai, W. Xu, K. Su, X. Li, D. Yuan, M. Hong, *Chem. Commun.* **2012**, *48*, 7456; d) F. Pointillart, K. Bernot, R. Sessoli, D. Gatteschi, *Chem. Eur. J.* **2007**, *13*, 1602; e) E. Colacio, J. Ruiz, A. J. Mota, M. A. Palacios, E. Cremades, E. Ruiz, F. J. White, E. K. Brechin, *Inorg. Chem.* **2012**, *51*, 5857.

[16] a) T. C. Stamatatos, S. J. Teat, W. Wernsdorfer, G. Christou, *Angew. Chem.* **2009**, *121*, 529; *Angew. Chem. Int. Ed.* **2009**, *48*, 521; b) V. Mereacre, A. M. Ako, R. Clérac, W. Wernsdorfer, I. J. Hewitt, C. E. Anson, A. K. Powell, *Chem. Eur. J.* **2008**, *14*, 3577; c) M. Li, Y. Lan, A. M. Ako, W. Wernsdorfer, C. E. Anson, G. Buth, A. K. Powell, Z. Wang, S. Gao, *Inorg. Chem.* **2010**, *49*, 11587; d) C. Papatriantafyllopoulou, K. A. Abboud, G. Christou, *Inorg. Chem.* **2011**, *50*, 8959; e) J.-L. Liu, F.-S. Guo, Z.-S. Meng, Y.-Z. Zheng, J.-D. Leng, M.-L. Tong, L. Ungur, L. F. Chibotaru, K. J. Heroux, D. N. Hendrickson, *Chem. Sci.* **2011**, *2*, 1268; f) H. Ke, L. Zhao, Y. Guoa, J. K. Tang, *Dalton Trans.* **2012**, *41*, 2314; g) V. Chandrasekhar, P. Bag, M. Speldrich, J. Leusen, P. Kögerler, *Inorg. Chem.* **2013**, *52*, 5035.

[17] a) G. J. Sopasis, M. Orfanoudaki, P. Zarmpas, A. Philippidis, M. Siczek, T. Lis, J. R. O'Brien, C. J. Milios, *Inorg. Chem.* **2012**, *51*, 1170; b) K. C. Mondal, A. Sundt, Y. Lan, G. E. Kostakis, O. Waldmann, L. Ungur, L. F. Chibotaru, C. E. Anson, A. K. Powell, *Angew. Chem.* **2012**, *124*, 7668; *Angew. Chem. Int. Ed.* **2012**, *51*, 7550; c) Y. Liu, Z. Chen, J. Ren, X. Q. Zhao, P. Cheng, B. Zhao, *Inorg. Chem.* **2012**, *51*, 7433; d) L.-F. Zou, L. Zhao, Y.-N. Guo, G.-M. Yu, Y. Guo, J. K. Tang, Y.-H. Li, *Chem. Commun.* **2011**, *47*, 8659; e) Y.-Z. Zheng, M. Evangelisti, R. E. P. Winpenny, *Chem. Sci.* **2011**, *2*, 99; f) V. Chandrasekhar, B. M. Pandian, J. J. Vittal, R. Clérac, *Inorg. Chem.* **2009**, *48*, 1148; g) V. Chandrasekhar, B. M. Pandian, R. Azhakar, J. J. Vittal, R. Clérac, *Inorg. Chem.* **2007**, *46*, 5140; h) T. Yamaguchi, J. P. Costes, Y. Kishima, M. Kojima, Y. Sunatsuki, N. Brefuel, J. P. Tuchagues, L. Vendier, W. Wernsdorfer, *Inorg. Chem.* **2010**, *49*, 9125.

[18] V. Chandrasekhar, A. Dey, A. J. Mota, E. Colacio, *Inorg. Chem.* **2013**, *52*, 4554.

[19] a) V. Chandrasekhar, R. Azhakar, B. Murugesapandian, T. Senapati, P. Bag, M. D. Pandey, S. K. Maurya, D. Goswami, *Inorg. Chem.* **2010**, *49*, 4008; b) V. Chandrasekhar, R. Azhakar, J. Bickley, A. Steiner, *Chem. Commun.* **2005**, 459; c) V. Chandrasekhar, R. Azhakar, G. T. S. Andavan, V. Krishnan, S. Zacchini, J. Bickley, A. Steiner, R. J. Butcher, P. Kögerler, *Inorg. Chem.* **2003**, *42*, 5989; d) V. Chandrasekhar, R. Azhakar, S. Zacchini, J. Bickley, A. Steiner, *Inorg. Chem.* **2005**, *44*, 4608; e) V. Chandrasekhar, R. Azhakar, B. M. Pandian, J. Bickley, A. Steiner, *Eur. J. Inorg. Chem.* **2008**, *7*, 1116; f) V. Chandrasekhar, B. M. Pandian, *Acc. Chem. Res.* **2009**, *42*, 1047.

[20] a) V. Chandrasekhar, B. M. Pandian, R. Boomishankar, A. Steiner, J. J. Vittal, A. Houri, R. Clérac, *Inorg. Chem.* **2008**, *47*, 4918; b) V. Chandrasekhar, B. M. Pandian, R. Boomishankar, A. Steiner, R. Clérac, *Dalton Trans.* **2008**, *38*, 5143.

[21] M. E. J. Lines, *J. Chem. Phys.* **1971**, *55*, 2977.

[22] J. P. Costes, F. Dahan, A. Dupuis, J. P. Laurent, *C. R. Acad. Sci., Ser. IIc* **1998**, *1*, 417.

[23] J. P. Costes, F. Dahan, J. Garcia Tojal, *Chem. Eur. J.* **2002**, *8*, 5430.

[24] E. Colacio, J. Ruiz, A. J. Mota, M. A. Palacios, E. Ruiz, E. Cremades, M. M. Hänninen, R. Sillanpää, E. K. Brechin, *C. R. Chim.* **2012**, *15*, 878.

[25] M. Towatari, K. Nishi, T. Fujinami, N. Matsumoto, Y. Sunatsuki, M. Kojima, N. Mochida, T. Ishida, N. Re, J. Mrozinski, *Inorg. Chem.* **2013**, *52*, 6160.

[26] L. Ungur, M. Thewissen, J.-P. Costes, W. Wernsdorfer, L. F. Chibotaru, *Inorg. Chem.* **2013**, *52*, 6328.

[27] a) J. Cirera, E. Ruiz, *C. R. Chim.* **2008**, *11*, 1227; b) G. Rajaraman, F. Totti, A. Bencini, A. Caneschi, R. Sessoli, D. Gatteschi, *Dalton Trans.* **2009**, 3153.

[28] a) S. K. Singh, N. K. Tibrewal, G. Rajaraman, *Dalton Trans.* **2011**, *40*, 10897.

[29] B. S. Furniss, A. J. Hannaford, P. W. G. Smith, A. R. Tatchell, *Vogel's Textbook of Practical Organic Chemistry*, 5th ed., ELBS, Longman, London, **1989**.

[30] a) *SMART & SAINT Software Reference manuals*, v.6.45, Bruker AXS, Madison, WI, **2003**; b) G. M. Sheldrick, *SADABS, a software for empirical absorption correction*, v.2.05, University of Göttingen, Germany, **2002**; c) *SHELXTL Reference Manual*, v.6.1, Bruker AXS, Madison, WI, **2000**; d) G. M. Sheldrick, *SHELXTL*, v.6.12, Bruker AXS, Madison, WI, **2001**; e) G. M. Sheldrick, *SHELXL97, Program for Crystal Structure Refinement*, University of Göttingen, Germany, **1997**; f) K. Bradenburg, *Diamond*, v.3.1eM, Crystal Impact GbR, Bonn, **2005**.

[31] a) R.-G. Xie, Z.-J. Zhang, J.-M. Yan, D.-Q. Yuan, *Synth. Commun.* **1994**, *24*, 53; b) E. Lambert, B. Chabut, S. Chardon-Noblat, A. Deronzier, G. Chottard, A. Bousseksou, J.-P. Tuchagues, J. Laugier, M. Bardet, J.-M. Latour, *J. Am. Chem. Soc.* **1997**, *119*, 9424.

[32] W. Huang, S. Gou, D. Hu, Q. Meng, *Synth. Commun.* **2000**, *30*, 1555.

Received: September 10, 2013
Published Online: November 26, 2013

